International Journal of Psychophysiology 166 (2021) 83–91

Contents lists available at ScienceDirect

International Journal of Psychophysiology

journal homepage: www.elsevier.com/locate/ijpsycho

A physiological and dynamical systems model of stress

Justin Brooks [a,b], Joshua C. Crone [c], Derek P. Spangler [d,*]

[a] D-Prime, LLC, United States of America
[b] University of Maryland, Baltimore County, Department of Computer Science and Electrical Engineering, United States of America
[c] CCDC-ARL, Computational and Information Sciences Directorate, United States of America
[d] The Pennsylvania State University, Department of Biobehavioral Health, United States of America

ARTICLE INFO

Keywords:
Stress
Cardiovascular
Computational modeling
Dynamical systems

ABSTRACT

Stress responses vary drastically for a given set of stimuli, individuals, or points in time. A potential source of this variance that is not well characterized arises from the theory of stress as a dynamical system, which implies a complex, nonlinear relationship between environmental/situational inputs and the development/experience of stress. In this framework, stress vs. non-stress states exist as attractor basins in a physiologic phase space. Here, we develop a model of stress as a dynamical system by coupling closed loop physiologic control to a dynamic oscillator in an attractor landscape. By characterizing the evolution of this model through phase space, we demonstrate strong sensitivity to the parameters controlling the dynamics and demonstrate multiple features of stress responses found in current research, implying that these parameters may contribute to a significant source of variability observed in empiric stress research.

1. Introduction

One of the primary areas of interest in stress research is the accurate identification and characterization of the experience of stress within and across individuals. There are many algorithms that attempt to classify/predict stress based on various features (e.g., facial expressions, body movement/gestures, and behavior), physiologic measures (e.g., blood pressure, skin conductance, and heart rate variability), and subjective report data (Bradley and Lang, 2000; Lee et al., 2011; Wagner et al., 2005). Despite several advances and impressive results with these approaches in specific circumstances, the development of a general method to estimate stress remains an open challenge. In part, this is because there is no "ground-truth" measure of stress. Often, researchers rely on subjective reporting or observed behavior to provide this information, although it is acknowledged that these are at best proxies to the underlying phenomena taking place. While our general inability to model stress may be related to a variable mapping between the actual state and the measures mentioned previously, we believe a more fundamental source of variance may be at play that has received less consideration.

Building upon the theoretical construct of emotional states as attractor basins in a dynamical, biological system, we postulate that the topology of the attractor landscape that contains these basins of attraction and the kinematic variables that control movement in the landscape are a significant source of variability (Oken et al., 2015; Wichers et al., 2015). In this construct, stress can be experienced at various levels of measurable observations. For example, stress can be experienced at a given blood pressure depending on the state of the dynamical system in which that observation arises.

In this manuscript, we introduce an idealized, mechanistic model that demonstrates this property. We believe that additional research in this area will ultimately yield improved estimates of emotional state that can be used to build adaptive technologies that respond to the emotional state of the individual and provide novel functionality.

Stress has evolved over eons to provide a compensatory response to permit advantageous and adaptive behaviors in response to some perturbation (LeDoux, 2012; Nesse, 1990). These responses manifest in multiple levels of organization, including peripheral physiology (i.e., viscera), the central nervous system (CNS), and the peripheral nervous system (PNS), including the autonomic nervous system (ANS) (Cacioppo et al., 1993; Critchley et al., 2003; Hagemann et al., 2003). Coordination among the component physiological systems has evolved to ensure that adequate metabolic requirements are met for impending behavior while also providing feedback signals to the CNS to facilitate the selection of appropriate behavior (Ochsner et al., 2009). Despite a conceptual/heuristic model of the CNS, PNS, ANS, and peripheral physiologic

* Corresponding author.
E-mail address: dpspang@psu.edu (D.P. Spangler).

https://doi.org/10.1016/j.ijpsycho.2021.05.005
Received 15 March 2021; Received in revised form 5 May 2021; Accepted 10 May 2021
Available online 23 May 2021

system interacting to generate the experience of stress, the characterization and quantification of this interaction, and therefore stress itself, remain a significant scientific hurdle. More recently, dynamic systems/ecological theories argue that "basic emotions are emergent phenomena that are the result of complex genetic and environmental interactions at all levels of organization" (Mason and Capitanio, 2012). In other words, these conceptual models consider the ANS, peripheral physiology, and CNS as a dynamical system that responds to the environment in which stress exists as a basin in the system's attractor landscape (Levenson, 2014; Mason and Capitanio, 2012; Oken et al., 2015; Scherer, 2009). Under this theoretical perspective, while stress arises as the result of a reflexive response to stimuli (providing some degree of specificity), there is variability in the development of stress that depends on the current state of the entire dynamical, biological system.

In this work, we move from heuristic to quantitative modeling of stress as a dynamical system. This is accomplished by developing a system of equations that couple closed loop physiologic control of blood pressure in response to the environment to an explicitly defined attractor landscape that quantitatively defines stress as a basin of attraction in its phase space. We use simulation to explore and characterize our model. First, we examine the model's response to a simulated stimulus and examine the stress response. Next, while fixing the physiologic response, we modify two parameters that control the system's dynamics and demonstrate that stress may or may not be experienced for a given stimulus and physiologic response. The first parameter that is varied is a potential energy (PE) difference between the fixed points at the centers of the basins of attraction. Changes in this parameter can manifest in many ways corresponding to both intra- and inter-subject variability. The second parameter is a damping coefficient, which can also account for intra- and inter-subject variability. For simplicity, we limit our model to two emotional states with a one-dimensional dynamical system and corresponding attractor landscape containing two basins of attraction. However, we emphasize that the fundamental theory behind the model presented in this work can be expanded to include more states by defining a higher-dimensional dynamical system with a higher-dimensional landscape and phase space. The results from our simulations and analysis demonstrate that the constructed model captures critical features that permeate the stress literature. Specifically, we demonstrate how emotional state can be predicted without specificity in stimulus or physiology by considering the complex dynamics of stress. Further, we provide a simple, mechanistic model that can account for varying emotional responses within and across individuals in empiric stress research.

2. Method

This section describes the model's constituent systems and presents the equations that compose the model. An apt metaphor for our model compares emotions to a ball rolling in a hilly terrain with multiple valleys (Oken et al., 2015; Wichers et al., 2015). The valleys represent states (one of which could be stress) and transitions are enabled by providing enough force to roll the ball over a hill and into another valley. The effect of the applied force on the ball is affected by kinematic parameters (e.g., damping/friction) and those that arise from the topology of the attractor landscape (e.g., steepness of the hill). Our work utilizes the simplest state transition model, a two-state simulation featuring two valleys with one hill separating them (see Fig. 1).

Consider, for example, an experiment where participants respond to a mental arithmetic task and baroreflex-mediated blood pressure changes and the perception of stress are observed (Callister et al., 1992; Forsman and Llndblad, 1983; Middlekauff et al., 1997). In the context of our metaphor, the Non-stressed state is represented by the left valley and the Stressed state[1] is represented by the right valley in Fig. 1. The length of time spent in a particular state and/or the point at which transition occurred would likely vary among individuals and be directly influenced by the kinematic and topological parameters mentioned previously.

This conceptualization is formalized through a set of equations. For presentation purposes, we first discuss the environment/physiologic interaction (i.e., mental arithmetic task) that gave rise to blood pressure control (through the baroreflex), then present the system of equations which represent emotion. In implementation, however, both of these component systems operate in parallel.

2.1. Blood pressure control through the baroreflex

In our simplified model of physiologic control, we extend existing equations that model the blood pressure response to baroreflex activity to incorporate closed-loop control (Ataee et al., 2014; Ottesen, 1997). The heart rate and blood pressure are determined through a pair of delay differential equations that compute blood pressure $P(t)$ and heart rate, $H(t)$ through:

$$\dot{H}(t) = \frac{\beta_H(t) T_s\left(P(t-\tau), \alpha_{sp}, P_{sp}\right)}{1+\gamma T_p\left(P(t), \alpha_{sp}, P_{sp}\right)} - V_H(t) T_p\left(P(t), \alpha_{sp}, P_{sp}\right) + \delta_H(H_0 - H(t)) \tag{1}$$

$$\dot{P}(t) = -\frac{P(t)}{R_a^0\left[1+\alpha T_s\left(P(t-\tau), \alpha_{sp}, P_{sp}\right)\right] C_a} + \frac{H(t)\Delta V}{C_a} \tag{2}$$

The nominal values of parameters α_{sp}, δ_H, H_0, ΔV, V_H, β_H, α, γ, C_a, R_a^0, and τ are taken from Ataee et al. (2014) and reported in Table 1. The sympathetic and parasympathetic tones as a function of blood pressure are represented by the sigmoidal-shaped functions $T_s(P(t-\tau), \alpha_{sp}, P_{sp}) = 1 - sig(P(t-\tau), \alpha_{sp}, P_{sp})$ and $T_p(P(t), \alpha_{sp}, P_{sp}) = sig(P(t), \alpha_{sp}, P_{sp})$, respectively, where $sig(x, a, b) = 1/(1+e^{-a(x-b)})$. In this work, the strength of the ANS tones V_H and β_H are held constant, but in reality are likely to change over various temporal scales according to multiple theories of autonomic system physiology (Berntson et al., 1991; Thayer and Lane, 2000, 2009). The sensitivity of the baroreflex for the sympathetic (T_s) and parasympathetic (T_p) activations are controlled by α_{sp} and P_{sp}, which control the steepness and center, respectively, of the activation curves.

For this dynamical systems model of emotion, the effect of internal and/or external stimuli manifests through $P^*(t)$. $P^*(t)$ is considered to be the output of a transfer function computed by the CNS that establishes dynamic physiologic set points in response to stimuli consistent with physiological models of allostasis in which physiologic set points vary to support dynamic functions (McEwen and Wingfield, 2003; Vernon et al., 2015). For example, this may represent an increase in the desired blood pressure to support cerebral perfusion changes occurring in response to a mental arithmetic task (Wang et al., 2005).

Fig. 2 shows the control architecture employed to drive the blood pressure toward P^*. The error between current $P(t)$ and $P^*(t)$ is defined as:

$$\Delta P(t) = P(t) - P^*(t) \tag{3}$$

where $\Delta P(t)$ is used to control the sensitivity of the baroreflex by shifting the position of its inflection point, P_{sp}, through:

$$\dot{P}_{sp}(t) = \Delta P(t)^* G \tag{4}$$

where G represents the gain on $\Delta P(t)$. Through this set of equations, the heart rate changes to meet $P^*(t)$ by changing the sensitivity of the

[1] For simplicity, when describing the states of the system we use the states of Non-stressed, Transition, and Stressed. However, these states could represent any number of possible emotions.

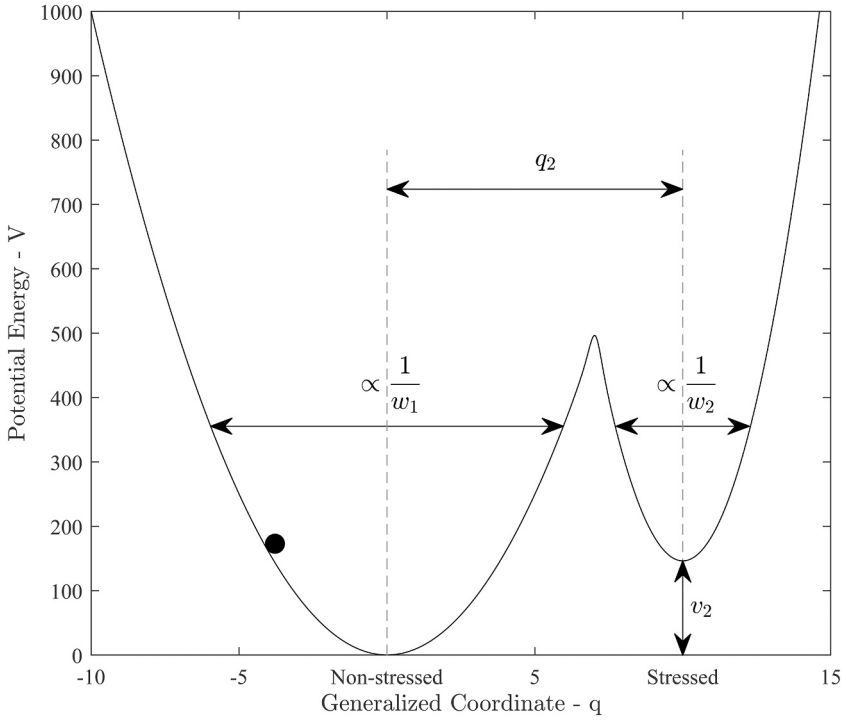

Fig. 1. The attractor landscape for $v_2 = 146.25$. The left basin represents a Non-stressed state and the right basin represents a Stressed state. q_2 is the horizontal distance between the two basins and w_1/w_2 are parameters that are inversely proportional to the width of the wells. The ball represents an instantaneous position of the system. A negative $\Delta P(t)$ pushes the ball toward the Stressed state.

Table 1
Parameters and variables used in our simulation. Many of the parameters for the baroreflex model are found in Ataee et al. (2014). However in addition to those parameters we provide descriptions of the parameters and variables introduced in this work.

Parameter	Value	Description
G	0.3	Gain for P_{sp} controller
τ	3 s	Time delay for sympathetic response
α_{sp}	0.07	Slope of sigmoid determining baroreflex response
ΔV	100 ml	Stroke volume
R_a^0	0.6 mm Hg s ml^{-1}	Minimum arterial resistance
C_a	1.55 ml mm Hg^{-1}	Arterial compliance
V_H	1.17 s^{-2}	Parasympathetic control of heart rate
β_H	0.84 s^{-2}	sympathetic control of heart rate
α	1.3	Sympathetic effect on R_a
γ	0.2	Parasympathetic damping of β_H
δ_H	1.7 s^{-1}	Relaxation time
q_0	Varies with V_2	Intersection point of two wells
w_1, w_2	10, 40	Inversely related to well width
q_2	10	Controls distance between two wells
c	Varies between 0 and 10	Damping of emotion transition
v_2	Varies between 0 and 975	Potential energy difference between two wells
f	17	Scaling term for forcing

baroreflex for the sympathetic (T_s) and parasympathetic (T_p) activations.

2.2. Model of emotion as a dynamical system

This section describes the attractor landscape that defines two states (Non-stressed and Stressed), the dynamics within the landscape, and its link to the closed-loop blood pressure control described above. We use the two-welled example as exemplified in Oken et al. (2015); Wichers et al. (2015) to define a two-basin potential landscape (V) shown in Fig. 1 and described by:

$$V(q) = [1 - sig(q, 10, q_0)]w_1 q^2 + sig(q, 10, q_0)\left[w_2(q - q_2)^2 + v_2\right]) \quad (5)$$

where w_1 and w_2 control the widths of the attractor basins, q_2 is the

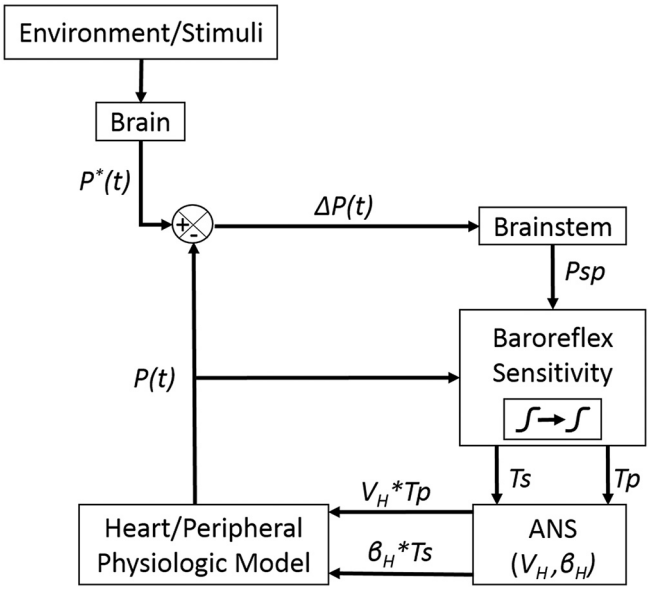

Fig. 2. Model of the closed loop control of blood pressure using the baroreflex. In this model, a blood pressure set point ($P^*(t)$) is determined by the brain in response to a stimulus. The actual blood pressure ($P(t)$) meets this set point by changing the sensitivity of the baroreflex (P_{sp}), which in turns amplifies or diminishes the influence of the ANS (parasympathetic (V_H), sympathetic (β_H)) on the heart rate. In turn, the heart rate changes blood pressure by decreasing or increasing cardiac output, which is directly related to the blood pressure.

distance between the basins, and v_2 is the difference in potential energy between basins (Fig. 1). In this set of equations, one emotion is centered at $q = 0$ and the other at q_2. For general purposes this could represent two disparate emotions (e.g., happy versus sad or aroused versus bored), or two similar emotions (e.g., happy and elated). In this work, state is quantitatively defined with respect to trajectory in or around these basins of attraction. There are three potential emotional states: 1. Non-stressed–stable trajectory around the left basin, 2. Transition–current trajectory spans both basins, and 3. Stressed–stable trajectory around the right basin. With respect to the widths (w_1 and w_2) larger values make the basins narrower, and therefore more force is required to transition to the other state. The sigmoid function (*sig*) is used for mixing the quadratic potentials to ensure $V(q)$ and dV/dq are smooth, and q_0 is obtained by determining the intersection of the two quadratics such that $0 < q_0 < q_2$.

While Eq. (5) describes the two-dimensional attractor landscape, the basins of attraction that characterize the stress states are defined in phase space. This phase space is characterized by q and $\dot{q}$, where q is the generalized coordinate of the oscillator and $\dot{q}$ is the velocity. The dynamics of this system are modeled as a driven oscillator such that:

$$\ddot{q} + c\dot{q} + \frac{dV}{dq} = -f\Delta P(t) \tag{6}$$

where c is the damping coefficient and f is a scaling parameter for the external forcing. Critically, $\Delta P(t)$ provides the force in the system and, depending on the other parameter values (including the topography of the attractor landscape (w_1, w_2, v_2, and q_2)), may cause the simulation to oscillate within a given state or to transition to another state (i.e., the other basin of attraction). In this work, we directly link the dynamical system of stress to the physiology given the known (albeit variable) correlation between physiology and stress. The parameter values for the simulations presented here are provided in Table 1.

2.3. Simulation strategy

In this work, we simulate experiments 180 s in duration, during which stimuli are presented for 5 s every 10 s starting at 20 s into the experiment. There are a total of 10 stimuli. Stimuli are represented by changes in $P^*(t)$ from a resting value of 84 mmHg to 92 mmHg, modeled after responses to a hard problem task in the literature (Middlekauff et al., 1997). The resulting step function for P^* is shown in Fig. 3a. After initializing the model, physiologic responses are determined through evolution of Eqs. (1)–(4) and the dynamics of the stress states are computed with Eq. (6). Stress state is then characterized over each peak-to-peak interval defining a half-period of oscillation. If q only spans the $(-\infty, q_0)$ domain over this interval, then we say the oscillation is contained in the left basin of attraction and the system is in the Non-stressed state. If, on the other hand, q only spans the (q_0, ∞) domain over this interval, then we say the oscillation is contained in the right basin of attraction and the system is in the Stressed state. If q spans both basins over a single peak-to-peak interval, then the system is determined to be in a Transition state. From these definitions, we are able to determine, for any given simulation, its initial state, the point at which it transitions states, and how long it remains in that state once transition has occurred.

It is particularly important to understand the potential influence of intra- and inter-individual differences and dynamics in the attractor landscape on emotional state, given the same stimuli and physiologic response. To that end, we systematically vary (i.e., linearly space) two parameters in the model: c from 0 to 10 and v_2 from 0 to 975. Twenty-one values of these parameters are used for a total of 441 simulations. Lower c values correspond to less damping and therefore increased lability (transitions between various states), since the opposing force that would attenuate the system's energy is reduced. Conceptually, this parameter could be linked to a variable like sleep quality given the empirical research suggesting that sleep quality is inversely related to emotional lability (Gujar et al., 2011a; Gujar et al., 2011b). Lower v_2 values reflect smaller differences in potential energy of the two basins. In this model, a smaller potential energy difference corresponds to a more

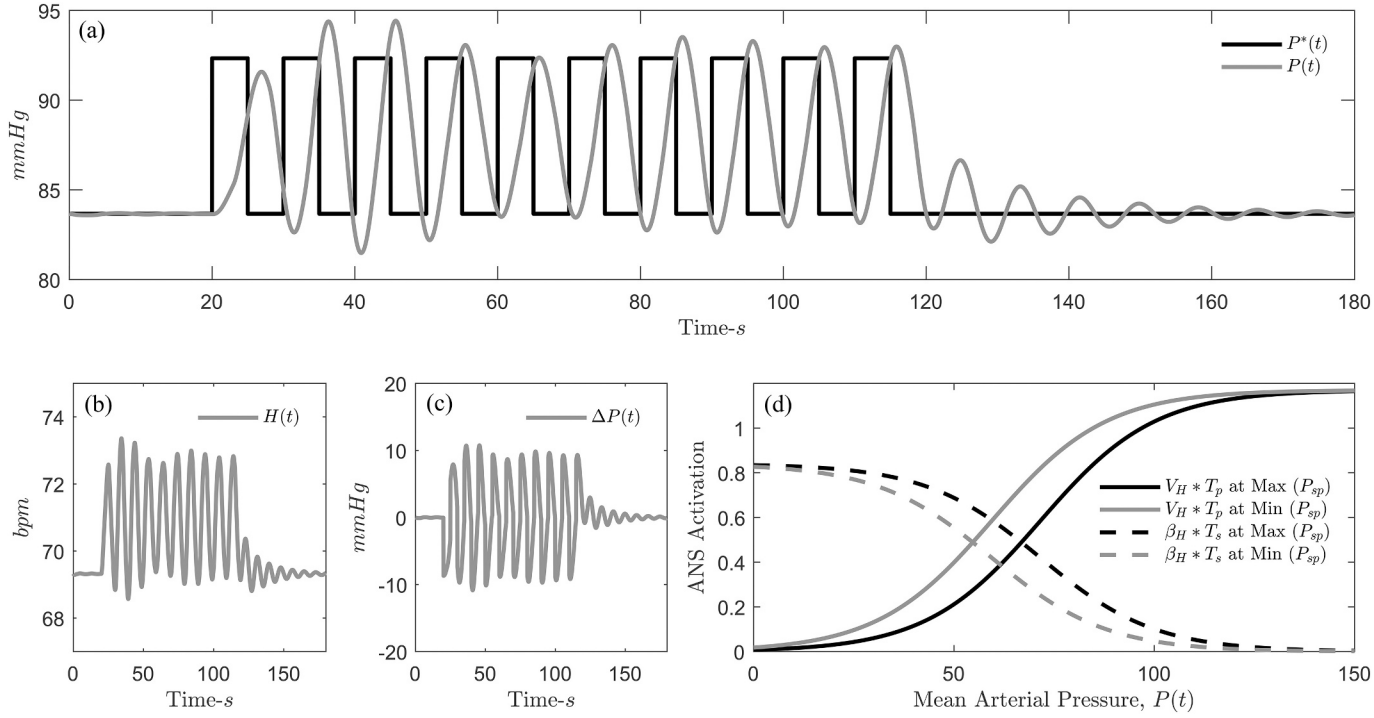

Fig. 3. The physiologic response is the same for all 441 simulations conducted in this study and is shown in plots a–d. As shown in plot a, blood pressure increases in response to the stimuli (modeled as $P^*(t)$, black line) by changing the heart rate (plot b). The error, $\Delta P(t)$ (plot c), is translated into baroreflex sensitivity by changing the inflection point (plot d) of the sigmoid that governs the gain on the ANS.

equal likelihood of residing in either state (Non-stressed vs. Stressed). Conversely, larger values of v_2 indicate that the system is less likely to enter or remain in the Stressed state. As an example application, in this context, v_2 could be reflective of the 5-HTT gene, consistent with the observation that these individuals with the short-arm variant tend to dwell in negative emotions when compared to long-arm genotype individuals (Caspi et al., 2003; Collier et al., 1996; Mendes de Oliveira et al., 1998; Pérez de Castro et al., 1999).

2.4. Analysis

Our analysis focuses on demonstrating that for a given physiologic response, multiple states are possible within a dynamical systems framework. We first analyze the time spent by our simulations in a given state in response to the stimuli. This is done using a percentage metric, which divides the time spent in a given state over the total time interval of interest. This is performed across the entire 180 s time series for each of the 441 combinations of c and v_2 parameter values.

Next, we analyze the temporal dynamics of the emotional state experience. We examine the number of simulations that experience their first and last Stress state across all the simulations as a function of time. This analysis is similar to survival analysis and the well-known Kaplan-Meier estimation technique (Kaplan and Meier, 1958).

Finally, the physiologic response in the model is correlated to the emotional states experienced for each simulation. This is accomplished by performing a cross-correlation with a lag of 3 s (related to $\tau = 3$ s) and taking the maximum value of the correlation as recommended by several emotion empiricists (Levenson, 2014; Mauss et al., 2005). The values considered in this analysis are $P^*(t)$, $V_H(t)$, $\beta_H(t)$, $P(t)$, and $H(t)$. The correlation coefficients are then transformed using *atanh* and subjected to a one-way Analysis of Variance (ANOVA) to determine if any of the measures show statistically significant differences in correlation with emotional state.

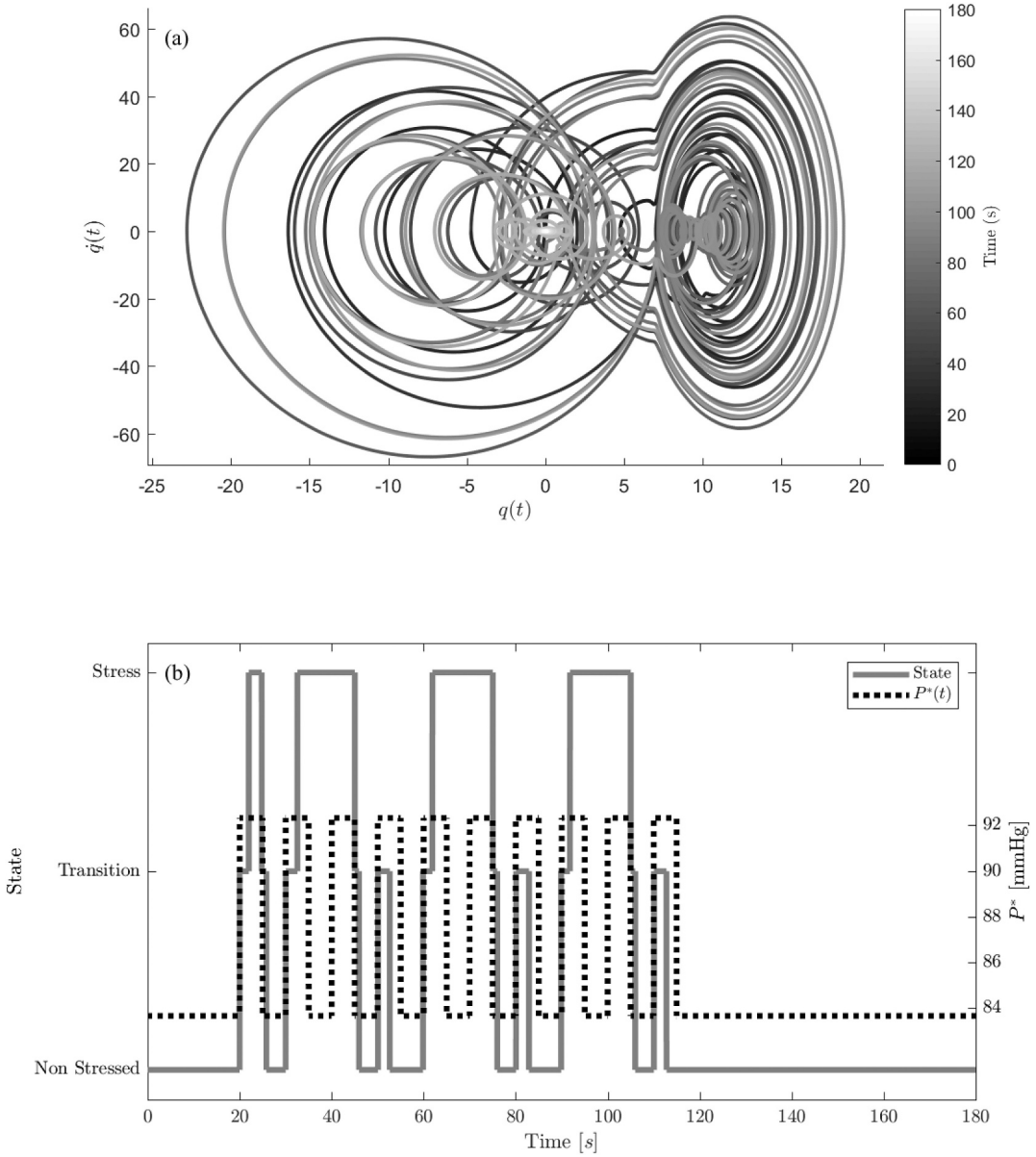

Fig. 4. In plot a, we graph the trajectory through phase space of the system for a full simulation of 10 stimuli, 180 s, with $v_2 = 146.25$ and $c = 0.5$. As shown in this figure, the system oscillates over several trajectories. In plot b, we graph the discretized values of state (dependent on the oscillations in plot b of Fig. 3) as a function of the stimuli. As shown in this figure, the experience of emotional state is not directly coupled to the experience of the stimuli.

3. Results

3.1. Physiology

The physiologic response for our simulated conditions is shown in Fig. 3. The stimuli are provided as a step function for $P^*(t)$ to which Eqs. (1)–(4) respond by attempting to reduce $\Delta P(t)$ to 0. As shown in Fig. 3a and b, the system responds within reasonable physiologic bounds to the presented stimuli. Mean arterial pressure, $P(t)$, ranges from 81.5 mmHg to 94.4 mmHg and the heart rate, $H(t)$, ranges from 68.5 bpm to 73.4 bpm. The difference between the desired and actual blood pressure, $\Delta P(t)$, is plotted in Fig. 3c and varies from −10.833 mmHg to 10.7286 mmHg. Through Eq. (4), changes to $P_{sp}(t)$ are driven by $\Delta P(t)$, which translates the baroreflex sensitivity curve to the right and left (corresponding to less versus more activity for a given $P(t)$). In these simulations, $P_{sp}(t)$ varies from 59.4 mmHg to 71.5 mmHg and the resulting range of activation curves, T_s and T_p, are illustrated in Fig. 3d. The time series of the autonomic, baroreflex activity is dependent on P_{sp}, as well as the instantaneous and delayed values of blood pressure, $P(t)$ and $P(t-\tau)$, respectively. The resulting time series of parasympathetic ($V_H * T_p(t)$) and sympathetic ($\beta_H * T_s(t)$) activations, which corresponds to rates of change in heart rate, ranges from 0.8766 to 1.0285 and 0.1016 to 0.2106, respectively. It is important to note that these physiologic dynamics are constant for all simulations in this work.

3.2. Emotion dynamics for a representative set of parameters

Fig. 4a shows the complete trajectory through phase space of an entire simulation, for parameters $v_2 = 146.25$ and $c = 0.5$. As shown in this figure, the trajectory through the phase space is complex, with oscillations centered at $q = 0$, $q = 10$, and across both basins of attraction. As discussed in the Methods section, this phase space was used to determine the discrete stress states being experienced by the simulation. Plot b of Fig. 4 charts stress state as defined in the Methods section against time and in reference to the stimuli. This data is for the simulation whose continuous trajectories in phase space are graphed in Fig. 4a. As shown in this plot, this simulation begins in the Non-stressed emotional state, then enters the Stressed emotional state in stimuli #1, #2, #3, #5, #6, #8, and #9. During the inter-trial intervals, the system experiences the Transition and Non-stressed emotional states, and finally resolves to the Non-stressed emotional state. The duration of these emotional states is ~3–7 s for this particular simulation, which is consistent with the emotion literature (Levenson, 2014; Scherer and Ekman, 2014). Not all simulations demonstrated this activity pattern, and were the focus of additional analyses.

3.3. Variability in the dynamics of emotion

Fig. 5 shows the amount of time spent in the Non-stressed, Transition, and Stressed emotional states for each parameter pair averaged across the entire 180 s. The variability across simulations ranged from 11.79% to 100% for the Non-stressed state, 0% to 71.43% for the Transition state, and 0% to 74.38% for the Stressed state. As evidenced by this quantitative analysis, there is marked heterogeneity in the states experienced by the different simulations, despite the fact that they simultaneously experienced the same stimuli and physiologic evolution. This variability arises strictly from changes in the dynamical system's parameters (c and v_2), which demonstrate nonlinear interactions as shown in Fig. 5.

A more complete characterization of the variability in state changes experienced by the simulations is provided by performing a modified survival analysis on the Stressed state. The results of this analysis are shown in Fig. 6. The black curve depicts when the first experience of stress occurred across the simulations. The median point in time (corresponding to 50% of the simulations) occurs at 31.31 s. However, as noted from this figure, some of the simulations experience the first Stressed state as early as 20.68 s or as late as 126.3 s seconds into the simulation, and some simulations do not experience the Stressed state at all. The gray curve depicts the time at which simulations experienced the Stressed state for the last time. The median value for this occurs at 114.8 s; however, some simulations experience this point as early as 24.88 s or as late as 138.2 s. This analysis demonstrates that differences in the attractor landscape generate significant variability in the time at which these simulations experience emotional states.

The final analysis examines the correlation between the physiologic time series data (including $P^*(t)$) and the emotional states to determine how well physiologic measures can be expected to predict emotional state in our model. As stated in the Methods section, this analysis uses a cross-correlation approach with a maximum lag of 3 s and records the maximum correlation value. The results of this analysis are plotted in Fig. 7. The correlation for each measures is as follows (mean ± standard deviation): $P^*(t)$: 0.5707 ± 0.3013, $V_H * T_p(t)$: 0.5567 ± 0.3000, $\beta_H * T_p(t)$: 0.5944 ± 0.3023, $P(t)$: 0.5694 ± 0.3015, and $H(t)$ 0.5640 ± 0.3009. A one-way ANOVA performed on the arc hyperbolic tangent transformed correlation coefficients revealed no significant difference between the physiologic parameter and degree of correlation to emotional state, $F(4,2204)=0.67, p=0.6144$.

4. Discussion

Our metric of stress state is discretized according to theories that regard these states as basins of attraction in phase space, wherein a complete oscillation around a basin or basins defines a state (Oken et al.,

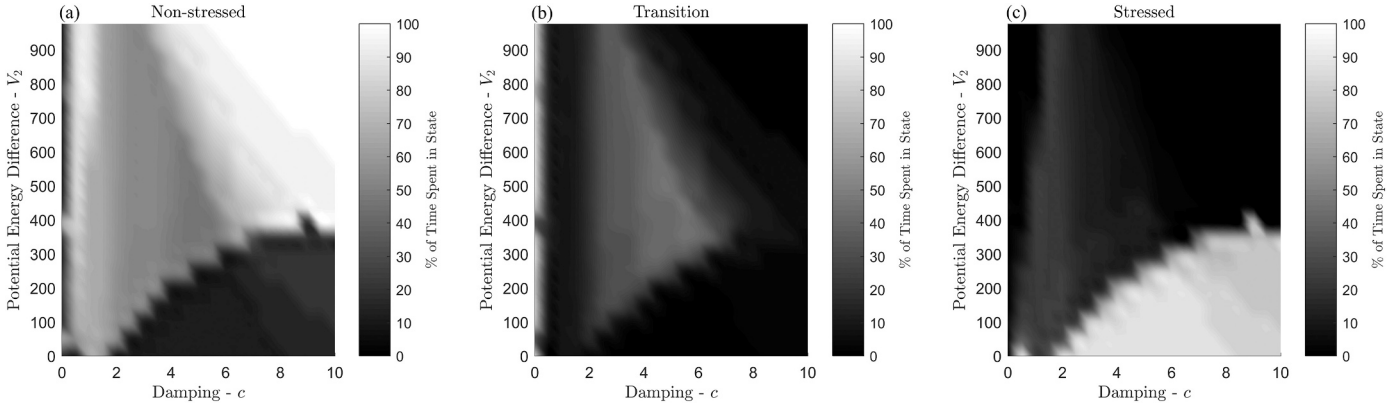

Fig. 5. Percentage of time spent in each possible state as a function of parameters v_2 and c. Of note, the physiologic response and stimuli experienced are always the same. As is shown in each plot, the time spent in each state is nonlinear and varies according to the value of v_2 and c.

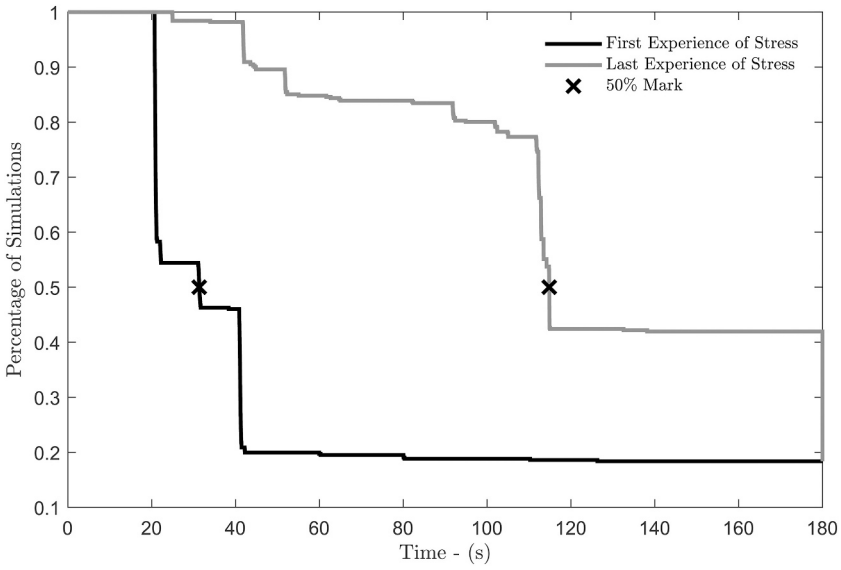

Fig. 6. Analysis of the first and last experience of the Stressed state. The black curve signifies the first experience of stress, which varies from very early (20.68 s) to very late (126.3 s) in the simulation. Half of the simulations experienced stress for the first time by 31.31 s (left, black x). The gray curve reflects the percentage of simulations that experienced the last Stress state. This occurred by 114.8 s for 50% of the simulations (right, black x); however, the range was 24.88 s to 138.2 s. (For reference, the first stimulus was experienced at 20 s and the last stimulus was experienced at 110 s, as in Fig. 4.)

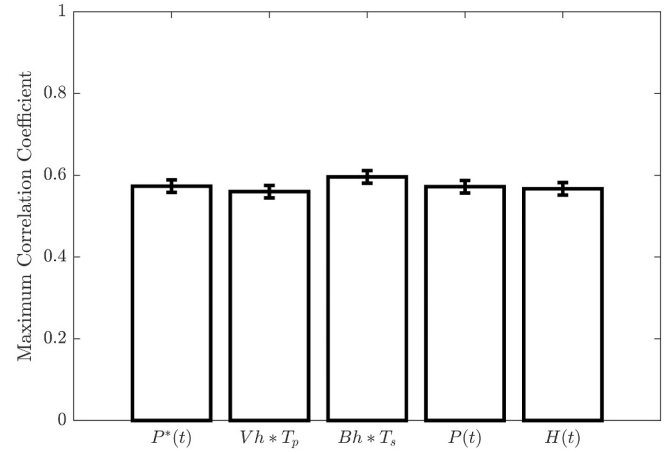

Fig. 7. The maximum, time-lagged correlation between physiologic measures and emotional state is similar across the various physiologic measures, and on average was 0.5701. One-way ANOVA revealed no statistically significant differences in the correlation between physiologic variables and emotional state across the 441 parameter value combinations.

2015). Using this approach, we are able to observe and quantify changes in stress state over time and across two parameters—one that changes the topography of the landscape (v_2) and one that affects the forces acting upon state transitions (c). Our dynamical systems model of state captures extant observations in stress research. Specifically, for a given physiologic response and stimuli frequency/magnitude, variability in the attractor landscape and/or dynamics can yield markedly different states. This variability can be construed as the effect of differences within (over time) and across individuals. Therefore, while none of the parameters used in this work are stochastic (although they could be modeled as such) the model generates a stable, non-deterministic mapping between physiology and stress states. This stability (which bounds the model) is enforced by the balance between damping and forcing functions in Eq. (6). To the best of our knowledge, this is the first mechanistic model to demonstrate this theoretical perspective. As such, it may prove valuable to researchers for evaluating and conceptualizing empirical data. In the first analysis, we characterize the duration of time spent in the stress states as a function of two parameters (c and v_2) that were varied in our model. As an example, we suggested these parameters could represent sleep quality and 5-HTT genotype as potential sources of state and trait level variability. However, these parameters and others in the model could be correlated with other sources of inter and intra-individual sources of variability. Regardless of their biological correlates, variation in these parameters yielded different stress responses (timing and quality) for a given stimulus and physiologic response.

Across all of the simulations, the baroreflex response to $\Delta P(t)$ is the same, despite the differences in the experienced emotional states that are described above. Therefore, the low correlation between the physiology simulated and the emotional states is expected. However, the average correlation observed in this study across all of the physiologic measures (including the stimulus $P^*(t)$) is 0.571, which is consistent with results found in the literature (Kreibig, 2010; Levenson, 2014; Mauss et al., 2005). This observation implies that approximately 67% of the variance in stress experience may be the result of the attractor landscape and its accompanying kinematics, rather than physiology or environmental stimuli.

Our research is consistent with the theoretical perspective that stress manifests as basins of attraction in a dynamical system and therefore inherently argues against physiologic specificity for a given stress state. More directly, this model argues that states and the transitions between them are a function of physiology, stimuli, attractor landscape topology, and the parameters that control dynamics between them. To date, most empirical work has focused on relating emotional state to physiology, behavior, and stimuli, with little attention being given to the parameters that influence the dynamics of emotion. The mechanistic model described here provides a parameterizable description of state that utilizes ANS activations to mediate the relationship between the CNS and physiology in a dynamical systems framework that can be utilized as a tool to further represent and understand stress state.

While the proposed model captures some generic features of current affective research, there are others that merit exploration. First, within the context of this model, several physiologic parameters affect the baroreflex as described in Ataee et al. (2014), including those related to the inherent delay of the sympathetic system, compliance of the arteries, and intrinsic rate of the sinoatrial node. In this work, we utilize the baroreflex strictly as a means for modeling a physiologic response, but there are many other sources of physiologic control (e.g., respiratory sinus arrhythmia, which could be modeled as oscillations in V_H). A further simplification that was assumed in this work was that the baroreflex response considered in this work changes its lateral position for closed loop control. Other potential control parameters could include the slope of the sigmoid, scaling/height, among others. Certainly, more complex control is at play in vivo, which can be added to our work.

Changes in these parameters will necessarily alter the physiologic responses determined in Eqs. (1) and (2) and will ultimately affect stress dynamics. There are additional parameters within Eqs. (4), (5), and (6) that can be explored beyond c and v_2 that were varied for purposes of this study. Finally, more complex model architectures could be imposed. In this work, we describe a one-way interaction between physiology and emotion; i.e., the force provided for emotional state transitions is provided by $\Delta P(t)$ through Eq. (6). In reality, it is likely that the topology of the attractor landscape (w_1, w_2, q_2, v_2) in Eq. (5) and perhaps the kinematic variables (c, f) in Eq. (6) are time-varying and functionally linked to previous states visited and/or to the evolution of the physiology, thereby providing some closed loop control. It is also likely that the dimensionality of the emotional state landscape is of higher order than that presented in this work. While arguments on this subject are ongoing, the number of "basic" emotions is likely greater than 2, which would require topology more complex than that presented in Fig. 4. A limitation of the approach described here is the complexity of the model system. While the presented model is the 'simplest' (i.e. a two state system) instantiation of the non-linear mapping between physiology and stress, it is likely that stress is expressed in a much higher order space with two or three way interactions. For example, another level of interaction could be closed-loop influences from previous stress states affecting the topography of the basins of attraction making it more or less difficult to experience that stress state in response to a stressor. This may reflect an important variable underlying stress resilience (Montpetit et al., 2010). Such additional complexity would then require significant amounts time-series data that adequately sampled the state-space in order to confirm the model. This will be the focus of our future work.

In this work, we made the specific design choice to define states as complete cycles (oscillations) within a basin of attraction, while trajectories that spanned both basins were considered to be transition states. This choice was motivated by our desire to differentiate stable trajectories within a state from transition-state trajectories. Alternative definitions of state could be used. For example, an instantaneous position of the generalized coordinate (e.g. q in Fig. 1). Such a definition would permit rapid state transitions (sub-second) depending on the frequency of the oscillator or a time-averaged value of q, where the temporal window size controls the frequency at which state transitions occur. However, these definitions of state are not consistent with the dynamical systems approach presented in this work, where the entire phase space (both q and $\dot{q}$) should be considered in the definition of state. Furthermore, the model's focus on >1 Hz state transitions (as opposed to changes on a millisecond-to-millisecond basis) are commensurate with stress-related cardiovascular changes that are typically examined in the cardiovascular stress literature (Cacioppo, 1998). While the brain is capable of rapidly processing stress-related stimuli on a millisecond basis, the relationship of these dynamics to autonomic and stress-related feeling states requires further clarification (Pace-Schott et al., 2019). Yet, the model is generalizable such that it can be used to model states that may have faster, or slower, temporal dynamics than the frequency of the oscillator.

Critical questions persist with this work, including how the attractor landscape and the parameters that control the dynamics of emotional state are developed, where they anatomically reside, and how they function physiologically. Candidate regions include the thalamus, central autonomic network, and other subcortical structures that have been implicated in CNS/ANS interactions (Critchley, 2005). Our model is a significant asset for answering these questions because it provides time series ($q(t)$ and $\dot{q}(t)$) that we would hypothesize are correlated to the neural activity that reflects emotional state.

5. Conclusion

We have introduced a parameterizable, mechanistic dynamical systems model of emotional state that embraces current theory on how emotion manifests through the interaction of multiple component subsystems. The proposed model demonstrates significant emotional state variability, for a fixed set of stimuli and a stereotyped physiologic response, that arises from parameters that govern the dynamics of emotional state. This model provides a tool to help investigators explore the dynamics of emotional state beyond measures of physiology and stimuli, and therefore may provide additional insight for affective science research.

Acknowledgments

This research was sponsored by the U.S. Army Research Laboratory's (ARL) Human Research and Engineering Directorate (HRED) and was accomplished under Cooperative Agreement Number W911NF-21-2-0108. The views and conclusions contained in this document are those of the authors and should not be interpreted as representing the official policies, either expressed or implied, of the U.S. Army Research Laboratory's (ARL) Human Research and Engineering Directorate. The U.S. Government is authorized to reproduce and distribute reprints for Government purposes notwithstanding any copyright notation herein.

References

Ataee, P., Hahn, J.-O., Dumont, G.A., Boyce, W.T., 2014. Noninvasive subject-specific monitoring of autonomic-cardiac regulation. IEEE Trans. Biomed. Eng. 61 (4), 1196–1207. Retrieved 2016-12-28, from.

Berntson, G.G., Cacioppo, J.T., Quigley, K.S., 1991. Autonomic determinism: the modes of autonomic control, the doctrine of autonomic space, and the laws of autonomic constraint. Psychol. Rev. 98 (4), 459–487. Retrieved 2017-01-03. https://doi.org/10.1037/0033-295X.98.4.459.

Bradley, M.M., Lang, P.J., 2000. Measuring emotion: behavior, feeling, and physiology. Cogn. Neurosci. Emot. 25, 49–59.

Cacioppo, J.T., 1998. Somatic Responses to Psychological Stress: The Reactivity Hypothesis.

Cacioppo, J.T., Klein, D.J., Berntson, G.G., Hatfield, E., 1993. The psychophysiology of emotion. In: Lewis, M., Haviland, J.M. (Eds.), Handbook of Emotions. Guilford Press, New York, NY, US, pp. 119–142.

Callister, R., Suwarno, N.O., Seals, D.R., 1992. Sympathetic activity is influenced by task difficulty and stress perception during mental challenge in humans. J. Physiol. 454 (1), 373–387. Retrieved 2018-01-19. https://doi.org/10.1113/jphysiol.1992.sp019269 (August).

Caspi, A., Sugden, K., Moffitt, T.E., Taylor, A., Craig, I.W., Harrington, H., Poulton, R., 2003. Influence of life stress on depression: moderation by a polymorphism in the 5-HTT gene. Science 301 (5631), 386–389. Retrieved 2017-07-03, from.

Collier, D.A., Stöber, G., Li, T., Heils, A., Catalano, M., Di Bella, D., Lesch, K.P., 1996. A novel functional polymorphism within the promoter of the serotonin transporter gene: possible role in susceptibility to affective disorders. Mol. Psychiatry 1 (6), 453–460 (December).

Critchley, H.D., 2005. Neural mechanisms of autonomic, affective, and cognitive integration. J. Comp. Neurol. 493 (1), 154–166. Retrieved 2017-04-21. https://doi.org/10.1002/cne.20749 (December).

Critchley, H.D., Mathias, C.J., Josephs, O., O'Doherty, J., Zanini, S., Dewar, B.-K., Dolan, R.J., 2003. Human cingulate cortex and autonomic control: converging neuroimaging and clinical evidence. Brain 126 (10), 2139–2152. Retrieved 2016-12-22, from.

Forsman, L., Llndblad, L.E., 1983. Effect of mental stress on baroreceptor-mediated changes in blood pressure and heart rate and on plasma catecholamines and subjective responses in healthy men and women. Psychosom. Med. 45 (5), 435 (October).

Gujar, N., McDonald, S.A., Nishida, M., Walker, M.P., 2011a. A role for REM sleep in recalibrating the sensitivity of the human brain to specific emotions. Cereb. Cortex 21 (1), 115–123. Retrieved 2017-05-17. https://doi.org/10.1093/cercor/bhq064 (January).

Gujar, N., Yoo, S.-S., Hu, P., Walker, M.P., 2011b. Sleep deprivation amplifies reactivity of brain reward networks, biasing the appraisal of positive emotional experiences. J. Neurosci. 31 (12), 4466–4474. Retrieved 2017-05-17. https://doi.org/10.1523/JNEUROSCI.3220-10.2011 (March).

Hagemann, D., Waldstein, S.R., Thayer, J.F., 2003. Central and autonomic nervous system integration in emotion. Brain Cogn. 52 (1), 79–87. Retrieved 2016-12-28, from.

Kaplan, E.L., Meier, P., 1958. Nonparametric estimation from incomplete observations. J. Am. Stat. Assoc. 53 (282), 457–481. Retrieved 2018-01-22. https://doi.org/10.1080/01621459.1958.10501452 (June).

Kreibig, S.D., 2010. Autonomic nervous system activity in emotion: a review. Biol. Psychol. 84 (3), 394–421. Retrieved 2018-01-04, from.

LeDoux, J.E., 2012. Evolution of human emotion. In: Progress in Brain Research, vol. 195. Elsevier, pp. 431–442. https://doi.org/10.1016/B978-0-444-53860-4.00021-0. Retrieved 2017-05-17, from. http://linkinghub.elsevier.com/retrieve/pii/B9780444538604000210.

Lee, C.-C., Mower, E., Busso, C., Lee, S., Narayanan, S., 2011. Emotion recognition using a hierarchical binary decision tree approach. Speech Comm. 53 (9), 1162–1171. Retrieved from.

Levenson, R.W., 2014. The autonomic nervous system and emotion. Emot. Rev. 6 (2), 100–112. Retrieved 2018-01-04. https://doi.org/10.1177/1754073913512003 (April).

Mason, W.A., Capitanio, J.P., 2012. Basic emotions: a reconstruction. Emot. Rev. 4 (3), 238–244. Retrieved 2016-12-27. https://doi.org/10.1177/1754073912439763 (July).

Mauss, I.B., Levenson, R.W., McCarter, L., Wilhelm, F.H., Gross, J.J., 2005. The tie that binds? Coherence among emotion experience, behavior, and physiology. Emotion 5 (2), 175–190. Retrieved 2017-09-27. https://doi.org/10.1037/1528-3542.5.2.175.

McEwen, B.S., Wingfield, J.C., 2003. The concept of allostasis in biology and biomedicine. Horm. Behav. 43 (1), 2–15. Retrieved 2016-12-29, from.

Mendes de Oliveira, J.R., Otto, P.A., Vallada, H., Lauriano, V., Elkis, H., Lafer, B., Zatz, M., 1998. Analysis of a novel functional polymorphism within the promoter region of the serotonin transporter gene (5-HTT) in Brazilian patients affected by bipolar disorder and schizophrenia. Am. J. Med. Genet. 81 (3), 225–227 (May).

Middlekauff, H.R., Nguyen, A.H., Negrao, C.E., Nitzsche, E.U., Hoh, C.K., Natterson, B.A., Moriguchi, J.D., 1997. Impact of acute mental stress on sympathetic nerve activity and regional blood flow in advanced heart failure: implications for 'triggering' adverse cardiac events. Circulation 96 (6), 1835–1842. Retrieved 2018-01-04. https://doi.org/10.1161/01.CIR.96.6.1835 (September).

Montpetit, M.A., Bergeman, C.S., Deboeck, P.R., Tiberio, S.S., Boker, S.M., 2010. Resilience-as-process: negative affect, stress, and coupled dynamical systems. Psychol. Aging 25 (3), 631.

Nesse, R.M., 1990. Evolutionary explanations of emotions. Hum. Nat. 1 (3), 261–289. Retrieved 2017-05-17. https://doi.org/10.1007/BF02733986 (September).

Ochsner, K.N., Ray, R.R., Hughes, B., McRae, K., Cooper, J.C., Weber, J., Gross, J.J., 2009. Bottom-up and top-down processes in emotion generation: common and distinct neural mechanisms. Psychol. Sci. 20 (11), 1322–1331. https://doi.org/10.1111/j.1467-9280.2009.02459.x (November).

Oken, B.S., Chamine, I., Wakeland, W., 2015. A systems approach to stress, stressors and resilience in humans. Behav. Brain Res. 282, 144–154. Retrieved 2016-12-27, from.

Ottesen, J.T., 1997. Modelling of the baroreflex-feedback mechanism with time-delay. J. Math. Biol. 36 (1), 41–63. https://doi.org/10.1007/s002850050089 (Nov 01).

Pace-Schott, E.F., Amole, M.C., Aue, T., Balconi, M., Bylsma, L.M., Critchley, H., et al., 2019. Physiological feelings. Neurosci. Biobehav. Rev. 103, 267–304.

Pérez de Castro, I., Ibáñez, A., Saiz-Ruiz, J., Fernández-Piqueras, J., 1999. Genetic contribution to pathological gambling: possible association between a functional DNA polymorphism at the serotonin transporter gene (5-HTT) and affected men. Pharmacogenetics 9 (3), 397–400 (June).

Scherer, K.R., 2009. Emotions are emergent processes: they require a dynamic computational architecture. Philos. Trans. R. Soc. B 364 (1535), 3459–3474. Retrieved 2016-12-07, from.

Scherer, K., Ekman, P., 2014. Approaches to Emotion. Taylor & Francis. Retrieved from. https://books.google.com/books?id=k0mhAwAAQBAJ.

Thayer, J.F., Lane, R.D., 2000. A model of neurovisceral integration in emotion regulation and dysregulation. J. Affect. Disord. 61 (3), 201–216. Retrieved 2017-01-03, from.

Thayer, J.F., Lane, R.D., 2009. Claude Bernard and the heart–brain connection: further elaboration of a model of neurovisceral integration. Neurosci. Biobehav. Rev. 33 (2), 81–88. Retrieved 2017-01-03, from.

Vernon, D., Lowe, R., Thill, S., Ziemke, T., 2015. Embodied cognition and circular causality: on the role of constitutive autonomy in the reciprocal coupling of perception and action. Front. Psychol. 6 https://doi.org/10.3389/fpsyg.2015.01660. Retrieved 2016-12-23, from. http://www.ncbi.nlm.nih.gov/pmc/articles/PMC4626623/ (October).

Wagner, J., Kim, J., Andre, E., 2005. From physiological signals to emotions: implementing and comparing selected methods for feature extraction and classification. In: 2005 IEEE International Conference on Multimedia and Expo, pp. 940–943. https://doi.org/10.1109/ICME.2005.1521579 (July).

Wang, J., Rao, H., Wetmore, G.S., Furlan, P.M., Korczykowski, M., Dinges, D.F., Detre, J. A., 2005. Perfusion functional MRI reveals cerebral blood flow pattern under psychological stress. Proc. Natl. Acad. Sci. 102 (49), 17804–17809. Retrieved 2018-01-19. https://doi.org/10.1073/pnas.0503082102 (December).

Wichers, M., Wigman, J.T.W., Myin-Germeys, I., 2015. Micro-level affect dynamics in psychopathology viewed from complex dynamical system theory. Emot. Rev. 7 (4), 362–367. https://doi.org/10.1177/1754073915590623.